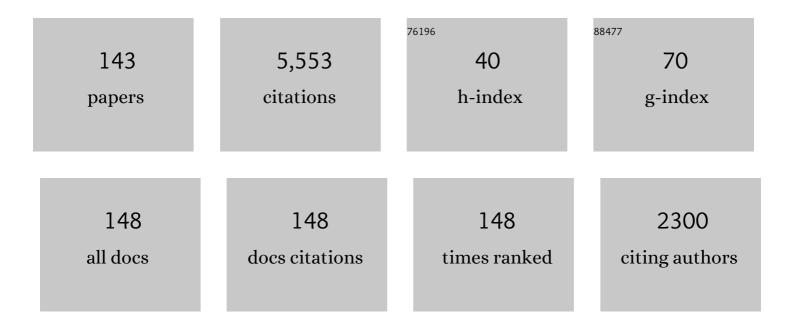
Goro Miyamoto

List of Publications by Year in descending order

Source: https://exaly.com/author-pdf/1436497/publications.pdf Version: 2024-02-01



#	Article	IF	CITATIONS
1	Stress–strain behavior of ferrite and bainite with nano-precipitation in low carbon steels. Acta Materialia, 2015, 83, 383-396.	3.8	297
2	Effects of transformation temperature on variant pairing of bainitic ferrite in low carbon steel. Acta Materialia, 2012, 60, 2387-2396.	3.8	264
3	Mapping the parent austenite orientation reconstructed from the orientation of martensite by EBSD and its application to ausformed martensite. Acta Materialia, 2010, 58, 6393-6403.	3.8	233
4	Accurate measurement of the orientation relationship of lath martensite and bainite by electron backscatter diffraction analysis. Scripta Materialia, 2009, 60, 1113-1116.	2.6	198
5	Carbon partitioning during quenching and partitioning heat treatment accompanied by carbide precipitation. Acta Materialia, 2015, 86, 137-147.	3.8	194
6	Effect of partitioning of Mn and Si on the growth kinetics of cementite in tempered Fe–0.6 mass% C martensite. Acta Materialia, 2007, 55, 5027-5038.	3.8	186
7	Precise measurement of strain accommodation in austenite matrix surrounding martensite in ferrous alloys by electron backscatter diffraction analysis. Acta Materialia, 2009, 57, 1120-1131.	3.8	174
8	Interaction of carbon partitioning, carbide precipitation and bainite formation during the Q&P process in a low C steel. Acta Materialia, 2016, 104, 72-83.	3.8	166
9	Effect of carbon content on variant pairing of martensite in Fe–C alloys. Acta Materialia, 2012, 60, 7265-7274.	3.8	161
10	Tensile Behavior of Ti,Mo-added Low Carbon Steels with Interphase Precipitation. ISIJ International, 2014, 54, 212-221.	0.6	125
11	Chemical boundary engineering: A new route toward lean, ultrastrong yet ductile steels. Science Advances, 2020, 6, eaay1430.	4.7	120
12	Microstructures and mechanical properties of metastable Ti–30Zr–(Cr, Mo) alloys with changeable Young's modulus for spinal fixation applications. Acta Biomaterialia, 2011, 7, 3230-3236.	4.1	119
13	Quantitative analysis of variant selection in ausformed lath martensite. Acta Materialia, 2012, 60, 1139-1148.	3.8	108
14	Multiphase Crystallography in the Nucleation of Intragranular Ferrite on MnS+V(C,N) Complex Precipitate in Austenite. ISIJ International, 2003, 43, 2028-2037.	0.6	104
15	Nucleation of Proeutectoid Ferrite on Complex Precipitates in Austenite. ISIJ International, 2003, 43, 1630-1639.	0.6	98
16	Crystallography of intragranular ferrite formed on (MnS+V(C,N)) complex precipitate in austenite. Scripta Materialia, 2003, 48, 371-377.	2.6	97
17	Variant Selection in Grain Boundary Nucleation of Upper Bainite. Metallurgical and Materials Transactions A: Physical Metallurgy and Materials Science, 2008, 39, 1003-1013.	1.1	97
18	Effects of Mn, Si and Cr addition on reverse transformation at 1073K from spheroidized cementite structure in Fe–0.6 mass% C alloy. Acta Materialia, 2010, 58, 4492-4502.	3.8	97

GORO MIYAMOTO

#	Article	IF	CITATIONS
19	Effects of transformation temperature on VC interphase precipitation and resultant hardness in low-carbon steels. Acta Materialia, 2015, 84, 375-384.	3.8	89
20	Orientation of austenite reverted from martensite in Fe-2Mn-1.5Si-0.3C alloy. Acta Materialia, 2018, 144, 601-612.	3.8	87
21	Direct measurement of carbon enrichment during austenite to ferrite transformation in hypoeutectoid Fe–2Mn–C alloys. Acta Materialia, 2013, 61, 3120-3129.	3.8	81
22	Interphase Precipitation of VC and Resultant Hardening in V-added Medium Carbon Steels. ISIJ International, 2011, 51, 1733-1739.	0.6	77
23	Growth mode of austenite during reversion from martensite in Fe-2Mn-1.5Si-0.3C alloy: A transition in kinetics and morphology. Acta Materialia, 2018, 154, 1-13.	3.8	77
24	Chemistry and three-dimensional morphology of martensite-austenite constituent in the bainite structure of low-carbon low-alloyÂsteels. Acta Materialia, 2018, 145, 154-164.	3.8	76
25	Effects of α/γ orientation relationship on VC interphase precipitation in low-carbon steels. Scripta Materialia, 2013, 69, 17-20.	2.6	68
26	Microstructure evolution during deformation of a near-α titanium alloy with different initial structures in the two-phase region. Scripta Materialia, 2009, 61, 419-422.	2.6	63
27	Direct measurement of carbon enrichment in the incomplete bainite transformation in Mo added low carbon steels. Acta Materialia, 2015, 91, 10-18.	3.8	63
28	Microstructure evolution during austenite reversion in Fe-Ni martensitic alloys. Acta Materialia, 2018, 144, 269-280.	3.8	61
29	Analysis of the mechanical behavior of a 0.3C-1.6Si-3.5Mn(wt%) quenching and partitioning steel. Materials Science & Engineering A: Structural Materials: Properties, Microstructure and Processing, 2016, 677, 505-514.	2.6	59
30	Variant selection in grain boundary nucleation of bainite in Fe-2Mn-C alloys. Acta Materialia, 2017, 127, 368-378.	3.8	59
31	Tensile Behavior of Ferrite-martensite Dual Phase Steels with Nano-precipitation of Vanadium Carbides. ISIJ International, 2015, 55, 1781-1790.	0.6	55
32	Quantitative measurements of phase equilibria at migrating α/γ interface and dispersion of VC interphase precipitates: Evaluation of driving force for interphase precipitation. Acta Materialia, 2017, 128, 166-175.	3.8	52
33	Nucleation of austenite from pearlitic structure in an Fe–0.6C–1Cr alloy. Scripta Materialia, 2009, 60, 485-488.	2.6	51
34	Three-dimensional atom probe analysis of boron segregation at austenite grain boundary in a low carbon steel - Effects of boundary misorientation and quenching temperature. Scripta Materialia, 2018, 154, 168-171.	2.6	51
35	Microstructure in a plasma-nitrided Fe–18 mass% Cr alloy. Acta Materialia, 2006, 54, 4771-4779.	3.8	50
36	Crystallographic Analysis of Proeutectoid Ferrite/Austenite Interface and Interphase Precipitation of Vanadium Carbide in Medium-Carbon Steel. Metallurgical and Materials Transactions A: Physical Metallurgy and Materials Science, 2013, 44, 3436-3443.	1.1	50

#	Article	IF	CITATIONS
37	Formation of grain boundary ferrite in eutectoid and hypereutectoid pearlitic steels. Acta Materialia, 2016, 103, 370-381.	3.8	50
38	Incomplete bainite transformation in Fe-Si-C alloys. Acta Materialia, 2017, 133, 1-9.	3.8	48
39	Variant selection of lath martensite and bainite transformation in low carbon steel by ausforming. Journal of Alloys and Compounds, 2013, 577, S528-S532.	2.8	47
40	Formation of ultrafine grained ferrite by warm deformation of lath martensite in low-alloy steels with different carbon content. Scripta Materialia, 2008, 59, 279-281.	2.6	42
41	Effects of Si and Cr on Bainite Microstructure of Medium Carbon Steels. ISIJ International, 2010, 50, 1476-1482.	0.6	42
42	Quantitative analysis of Mo solute drag effect on ferrite and bainite transformations in Fe-0.4C-0.5Mo alloy. Acta Materialia, 2019, 177, 187-197.	3.8	42
43	Quantitative measurement of carbon content in Fe–C binary alloys by atom probe tomography. Scripta Materialia, 2012, 67, 999-1002.	2.6	41
44	Effects of Ferrite Growth Rate on Interphase Boundary Precipitation in V Microalloyed Steels. ISIJ International, 2012, 52, 616-625.	0.6	40
45	Quantitative analysis of three-dimensional morphology of martensite packets and blocks in iron-carbon-manganese steels. Journal of Alloys and Compounds, 2013, 577, S587-S592.	2.8	40
46	A quantitative investigation of the effect of Mn segregation on microstructural properties of quenching and partitioning steels. Scripta Materialia, 2017, 137, 27-30.	2.6	40
47	Distribution of Dislocations in Nanostructured Bainite. Solid State Phenomena, 0, 172-174, 117-122.	0.3	39
48	Microstructural evaluation of austenite reversion during intercritical annealing of Fe–Ni–Mn martensitic steel. Journal of Alloys and Compounds, 2013, 577, S572-S577.	2.8	36
49	Incomplete transformation of upper bainite in Nb bearing low carbon steels. Materials Science and Technology, 2010, 26, 392-397.	0.8	35
50	Precipitation of nanosized nitrides in plasma nitrided Fe–M (M = Al, Cr, Ti, V) alloys. Materials Science and Technology, 2011, 27, 742-746.	0.8	34
51	Reconstruction of Parent Austenite Grain Structure Based on Crystal Orientation Map of Bainite with and without Ausforming. ISIJ International, 2011, 51, 1174-1178.	0.6	33
52	Kinetics of Reverse Transformation from Pearlite to Austenite in an Fe-0.6ÂMassÂpct C Alloy and the Effects of Alloying Elements. Metallurgical and Materials Transactions A: Physical Metallurgy and Materials Science, 2011, 42, 1586-1596.	1.1	33
53	Phase transformation mechanisms during Quenching and Partitioning of a ductile cast iron. Acta Materialia, 2019, 179, 1-16.	3.8	32
54	Thermomechanical Processing of Steel –Past, Present and Future–. Tetsu-To-Hagane/Journal of the Iron and Steel Institute of Japan, 2014, 100, 1062-1075.	0.1	29

#	Article	IF	CITATIONS
55	Role of cementite and retained austenite on austenite reversion from martensite and bainite in Fe-2Mn-1.5Si-0.3C alloy. Acta Materialia, 2021, 209, 116772.	3.8	27
56	Visible light response of nitrogen and sulfur co-doped TiO2 photocatalysts fabricated by anodic oxidation. Catalysis Today, 2011, 164, 399-403.	2.2	26
57	Fe-Fe3C binary phase diagram in high magnetic fields. Journal of Alloys and Compounds, 2015, 632, 251-255.	2.8	25
58	Analysis of recrystallization behavior of hot-deformed austenite reconstructed from electron backscattering diffraction orientation maps of lath martensite. Scripta Materialia, 2016, 112, 92-95.	2.6	25
59	Unraveling the effects of Nb interface segregation on ferrite transformation kinetics in low carbon steels. Acta Materialia, 2021, 215, 117081.	3.8	25
60	Key Factors in Grain Refinement of Martensite and Bainite. Materials Science Forum, 0, 638-642, 3044-3049.	0.3	23
61	Variant selection of lenticular martensite by ausforming. Scripta Materialia, 2012, 67, 324-327.	2.6	22
62	Crystallography and Interphase Boundary of Martensite and Bainite in Steels. Metallurgical and Materials Transactions A: Physical Metallurgy and Materials Science, 2017, 48, 2739-2752.	1.1	22
63	Crystallographic Restriction in Martensite and Bainite Transformations in Steels. Nippon Kinzoku Gakkaishi/Journal of the Japan Institute of Metals, 2015, 79, 339-347.	0.2	21
64	Characterization of Transformation Stasis in Low-Carbon Steels Microalloyed with B and Mo. Metallurgical and Materials Transactions A: Physical Metallurgy and Materials Science, 2014, 45, 5990-5996.	1.1	20
65	A comparative study on intrinsic mobility of incoherent and semicoherent interfaces during the austenite to ferrite transformation. Scripta Materialia, 2020, 188, 59-63.	2.6	20
66	Surface Hardening and Nitride Precipitation in the Nitriding of Fe-M1-M2 Ternary Alloys Containing Al, V, or Cr. Metallurgical and Materials Transactions A: Physical Metallurgy and Materials Science, 2015, 46, 5011-5020.	1.1	19
67	Carbon Enrichment in Austenite During Bainite Transformation in Fe-3Mn-C Alloy. Metallurgical and Materials Transactions A: Physical Metallurgy and Materials Science, 2015, 46, 1544-1549.	1.1	19
68	Carbon enrichment during ferrite transformation in Fe-Si-C alloys. Acta Materialia, 2018, 149, 68-77.	3.8	19
69	Analysis of the interaction between moving $\hat{I}\pm/\hat{I}^3$ interfaces and interphase precipitated carbides during cyclic phase transformations in a Nb-containing Fe-C-Mn alloy. Acta Materialia, 2018, 158, 167-179.	3.8	19
70	Interaction of Alloying Elements with Migrating Ferrite/Austenite Interface. ISIJ International, 2020, 60, 2942-2953.	0.6	19
71	Excess Carbon Enrichment in Austenite During Intercritical Annealing. Metallurgical and Materials Transactions A: Physical Metallurgy and Materials Science, 2013, 44, 4872-4875.	1.1	18
72	Plasma Nitriding Behavior of Fe-C-M (MÂ=ÂAl, Cr, Mn, Si) Ternary Martensitic Steels. Metallurgical and Materials Transactions A: Physical Metallurgy and Materials Science, 2014, 45, 239-249.	1.1	18

#	Article	IF	CITATIONS
73	Weak influence of ferrite growth rate and strong influence of driving force on dispersion of VC interphase precipitation in low carbon steels. Acta Materialia, 2020, 186, 533-544.	3.8	18
74	Effect of Alloying Elements on the High-Temperature Tempering of Fe-0.3N Martensite. Acta Materialia, 2021, 206, 116612.	3.8	17
75	Volume Fractions of Proeutectoid Ferrite/Pearlite and Their Dependence on Prior Austenite Grain Size in Hypoeutectoid Fe-Mn-C Alloys. Metallurgical and Materials Transactions A: Physical Metallurgy and Materials Science, 2013, 44, 5456-5467.	1.1	16
76	Effect of Ferrite/Martensite Phase Size on Tensile Behavior of Dual-Phase Steels with Nano-Precipitation of Vanadium Carbides. Metallurgical and Materials Transactions A: Physical Metallurgy and Materials Science, 2019, 50, 4111-4126.	1.1	15
77	Effects of Pre-tempering on Intercritical Annealing in Fe-2Mn-0.3C Alloy. Metallurgical and Materials Transactions A: Physical Metallurgy and Materials Science, 2014, 45, 5290-5294.	1.1	14
78	Atom Probe Compositional Analysis of Interphase Precipitated Nano-Sized Alloy Carbide in Multiple Microalloyed Low-Carbon Steels. Microscopy and Microanalysis, 2019, 25, 447-453.	0.2	14
79	Effects of Mo on Carbon Enrichment During Proeutectoid Ferrite Transformation in Hypoeutectoid Fer-C-Mn Alloys. Metallurgical and Materials Transactions A: Physical Metallurgy and Materials Science, 2015, 46, 2347-2351.	1.1	13
80	Randomization of Ferrite/austenite Orientation Relationship and Resultant Hardness Increment by Nitrogen Addition in Vanadium-microalloyed Low Carbon Steels Strengthened by Interphase Precipitation. ISIJ International, 2018, 58, 542-550.	0.6	13
81	Microstructures and tensile properties of friction stir welded 0.2%C–Si–Mn steel. Materials Science & Engineering A: Structural Materials: Properties, Microstructure and Processing, 2021, 799, 140068.	2.6	13
82	Comparison of Variant Selection between Lenticular and Lath Martensite Transformed from Deformed Austenite. ISIJ International, 2013, 53, 915-919.	0.6	12
83	Effects of Heating Rate on Formation of Globular and Acicular Austenite during Reversion from Martensite. Metals, 2019, 9, 266.	1.0	12
84	Microstructure of reverted austenite in Fe-0.3N martensite. Scripta Materialia, 2018, 156, 85-89.	2.6	11
85	Solute cluster-induced precipitation and resultant surface hardening during nitriding of Fe–Al–V alloys. Scripta Materialia, 2021, 203, 114121.	2.6	11
86	Enhanced hardening by multiple microalloying in low carbon ferritic steels with interphase precipitation. Scripta Materialia, 2022, 212, 114558.	2.6	11
87	Nanosized Cr-N clustering in expanded austenite layer of low temperature plasma-nitrided Fe-35Ni-10Cr alloy. Scripta Materialia, 2022, 213, 114637.	2.6	11
88	Crystallography of Ferrite Nucleation at Austenite Grain Boundary in a Low Carbon Steel. Materials Science Forum, 0, 654-656, 7-10.	0.3	10
89	Microstructure of Pure Iron Treated by Nitriding and Quenching Process. Nippon Kinzoku Gakkaishi/Journal of the Japan Institute of Metals, 2012, 76, 256-264.	0.2	10
90	Anisotropic Ferrite Growth and Substructure Formation during Bainite Transformation in Fe-9Ni-C Alloys: <i>In-Situ</i> Measurement. Materials Transactions, 2018, 59, 214-223.	0.4	10

Goro Μιγαμοτο

#	Article	lF	CITATIONS
91	Resistance to Temper Softening of Low Carbon Martensitic Steels by Microalloying of V, Nb and Ti. ISIJ International, 2021, 61, 1641-1649.	0.6	10
92	Formation of Ultrafine Grained Ferrite by Warm Deformation of Tempered Lath Martensite in Low Alloy Steels. Materials Science Forum, 2007, 558-559, 557-562.	0.3	9
93	Three-dimensional observations of morphology of low-angle boundaries in ultra-low carbon lath martensite. Journal of Electron Microscopy, 2017, 66, 380-387.	0.9	9
94	Relationship between mechanical response and microscopic crack propagation behavior of hydrogen-related intergranular fracture in as-quenched martensitic steel. Materials Science & Engineering A: Structural Materials: Properties, Microstructure and Processing, 2022, 831, 142288.	2.6	9
95	Multi-scale three-dimensional analysis on local arrestability of intergranular crack in high-strength martensitic steel. Acta Materialia, 2022, 234, 118053.	3.8	9
96	Improvement of Strength and Ductility of Steels Using Nano-precipitation. Materia Japan, 2015, 54, 3-11.	0.1	8
97	Banding effects on the process of grain refinement by cold deformation and recrystallization of acicular C-Mn steel. Materials Science & Engineering A: Structural Materials: Properties, Microstructure and Processing, 2017, 697, 1-7.	2.6	8
98	Comparative Study of VC, NbC, and TiC Interphase Precipitation in Microalloyed Low-carbon Steels. Metallurgical and Materials Transactions A: Physical Metallurgy and Materials Science, 2020, 51, 6149-6158.	1.1	8
99	Formation of abnormal nodular ferrite with interphase precipitation in a vanadium microalloyed low carbon steel. Scripta Materialia, 2021, 198, 113823.	2.6	8
100	Current Understanding of Microstructure and Properties of Micro-Alloyed Low Carbon Steels Strengthened by Interphase Precipitation of Nano-Sized Alloy Carbides: A Review. Jom, 2021, 73, 3214-3227.	0.9	8
101	Lattice Strain and Strength Evaluation on V Microalloyed Pearlite Steel. ISIJ International, 2020, 60, 1810-1818.	0.6	7
102	Phase separation with ordering in aged Fe-Ni-Mn medium entropy alloy. Acta Materialia, 2022, 223, 117487.	3.8	7
103	Precipitation in Plasma Nitrided Fe-M(M=Ti, V, Al) Alloys. Materials Science Forum, 2005, 492-493, 539-544.	0.3	6
104	Microstructure and Growth Kinetics of Nitrided Zone in Plasma-nitrided Fe–Cr Alloys. ISIJ International, 2007, 47, 1491-1496.	0.6	6
105	Crystallography of Martensitic and Bainitic Transformation in Steels. Materia Japan, 2010, 49, 332-336.	0.1	6
106	Effects of Si and Cr on Bainite Microstructure of Medium Carbon Steels. Tetsu-To-Hagane/Journal of the Iron and Steel Institute of Japan, 2010, 96, 392-399.	0.1	6
107	Continuous Dynamic Recrystallization during Warm Deformation of Tempered Lath Martensite in a Medium Carbon Steel. Key Engineering Materials, 0, 508, 124-127.	0.4	6
108	Effect of Titanium Carbide Inclusions on Morphology of Low-Carbon Steel Martensite. Materials Science Forum, 2013, 738-739, 25-30.	0.3	6

#	Article	IF	CITATIONS
109	Tensile Behavior of Ti,Mo-Added Low Carbon Steels with Interphase Boundary Precipitated Structures. Tetsu-To-Hagane/Journal of the Iron and Steel Institute of Japan, 2013, 99, 352-361.	0.1	6
110	Effect of Forging Temperature on Microstructure Evolution and Tensile Properties of Ti-17 Alloys. Materials Transactions, 2019, 60, 1733-1739.	0.4	6
111	Grain Refinement by Cyclic Displacive Forward/Reverse Transformation in Fe-High-Ni Alloys. Metallurgical and Materials Transactions A: Physical Metallurgy and Materials Science, 2017, 48, 4204-4210.	1.1	5
112	Effects of Alloying Elements on Microstructure, Hardness and Growth Rate of Compound Layer in Gaseous-Nitrided Ferritic Alloys. Materials Transactions, 2021, 62, 596-602.	0.4	5
113	Improvement of Strength–Ductility Balance by the Simultaneous Increase in Ferrite and Martensite Strength in Dual-Phase Steels. Metallurgical and Materials Transactions A: Physical Metallurgy and Materials Science, 2021, 52, 5394-5408.	1.1	5
114	Formation of Martensite Austenite Constituent in Continuously Cooled Nb-Bearing Low Carbon Steels. Materials Science Forum, 2010, 638-642, 3080-3085.	0.3	4
115	Microstructure and Mechanical Properties of Austempered Medium Carbon Steels. Tetsu-To-Hagane/Journal of the Iron and Steel Institute of Japan, 2011, 97, 26-33.	0.1	4
116	Erratum to "Tensile Behavior of Ti,Mo-added Low Carbon Steels with Interphase Precipitation―[ISIJ Int. 54(1): 212-221 (2014)]. ISIJ International, 2014, 54, 474-474.	0.6	4
117	EFFECTS OF Mn AND Si ADDITIONS ON PEARLITE-AUSTENITE PHASE TRANSFORMATION IN Fe0.6C STEEL. Jinshu Xuebao/Acta Metallurgica Sinica, 2010, 46, 1066-1074.	0.3	4
118	Interphase Boundary Precipitation of VC Accompanying Ferrite and Pearlite Transformation in Medium Carbon Steels. Solid State Phenomena, 0, 172-174, 420-425.	0.3	3
119	Effects of Transformation Temperature on Variant Grouping of Bainitic Ferrite in Low Carbon Steel. Solid State Phenomena, 0, 172-174, 155-160.	0.3	3
120	Model for Predicting Phase Transformation and Yield Strength of Vanadium Microalloyed Carbon Steels. ISIJ International, 2012, 52, 669-678.	0.6	3
121	Lattice Strain and Strength Evaluation on V Microalloyed Pearlite Steel. Tetsu-To-Hagane/Journal of the Iron and Steel Institute of Japan, 2018, 104, 673-682.	0.1	3
122	Roles of transformation interfaces in the design of advanced high strength steels. IOP Conference Series: Materials Science and Engineering, 2019, 580, 012005.	0.3	3
123	Surface Hardening and Precipitation Behaviors in Plasma-nitrided Fe-(2- <i>x</i>) at%Al- <i>x</i> at%Ti Alloys. Tetsu-To-Hagane/Journal of the Iron and Steel Institute of Japan, 2019, 105, 324-333.	0.1	3
124	Formation Mechanism of Coarse Austenite Grain during Hot Forging and Cooling in Case Hardening Steel. Tetsu-To-Hagane/Journal of the Iron and Steel Institute of Japan, 2020, 106, 108-120.	0.1	3
125	Nano Clustering of Interstitial and Substitutional Solute Atoms in Steels. Materia Japan, 2020, 59, 128-133.	0.1	3
126	Nitrogen-Induced Phase Separation in Equiatomic FeNiCo Medium Entropy Alloy. Metallurgical and Materials Transactions A: Physical Metallurgy and Materials Science, 2022, 53, 3216-3223.	1.1	3

#	Article	IF	CITATIONS
127	Effects of Pre-exsisting Boundaries on Microstructure Obtained by Plasma-nitriding of Fe–18%Cr Alloy. ISIJ International, 2009, 49, 1801-1805.	0.6	2
128	Alloying Effects on Reverse Transformation to Austenite from Pearlite or Tempered Martensite Structures. Materials Science Forum, 2010, 638-642, 3400-3405.	0.3	2
129	Ferrite Transformation from Fe-0.3N Austenite. ISIJ International, 2021, 61, 343-349.	0.6	2
130	Effect of Deformation Temperature, Strain Rate, and Strain on the Microstructure Evolution of Ti-17 Alloy. Metallurgical and Materials Transactions A: Physical Metallurgy and Materials Science, 2021, 52, 3107-3121.	1.1	2
131	Microstructure formation during thermomechanical processing in Ti-17 alloy. MATEC Web of Conferences, 2020, 321, 12006.	0.1	2
132	Age-Hardening Behavior in High-Nitrogen Stable Austenitic Stainless Steel. Materials Transactions, 2022, 63, 163-169.	0.4	2
133	Influence of Acicular Ferrite Microstructure on Toughness of Ti-Rare Earth Metal (REM)-Zr Killed Steel. Tetsu-To-Hagane/Journal of the Iron and Steel Institute of Japan, 2022, 108, 295-305.	0.1	2
134	Precipitation Modeling in Nitriding in Fe-M Binary System. Metallurgical and Materials Transactions A: Physical Metallurgy and Materials Science, 2016, 47, 4970-4978.	1.1	1
135	Resistance to Temper Softening of Low Carbon Martensitic Steels by Microalloying of V, Nb and Ti. Tetsu-To-Hagane/Journal of the Iron and Steel Institute of Japan, 2020, 106, 362-371.	0.1	1
136	Hardening Behavior in Diffusion Zone of Fe–Mn and Fe–Cr Binary Alloys Nitrocarburized after Cold Working. ISIJ International, 2022, 62, 209-217.	0.6	1
137	Effect of Deformation Prior to Nitriding on Microstructure and Hardness Behavior in Plasma-Nitrided Ferritic Alloys. Materials Transactions, 2022, 63, 864-871.	0.4	1
138	Hot Deformation Behavior of Near-α Ti-Fe Alloy in (α+β) Two-Phase Region with Different Fe Content. Materials Science Forum, 2010, 638-642, 310-314.	0.3	0
139	Analysis of Recrystallization Behavior of Hot-Deformed Austenite Reconstructed from EBSD Orientation Maps of Lath Martensite. Materials Science Forum, 2016, 879, 2389-2394.	0.3	0
140	Crystal Orientation Relationships among Acicular Ferrite, Oxide and the Austenite Matrix in a Steel Weld Metal. Materials Science Forum, 0, 1016, 1014-1018.	0.3	0
141	Introduction: New and Improved Steels. , 2022, , 1-2.		0
142	Strengthening of Steels by Nano-sized Precipitation. Journal of the Japan Society for Technology of Plasticity, 2013, 54, 873-876.	0.0	0
143	Effect of Alloying Elements on the High-Temperature Tempering of Fe-0.3N Martensite. SSRN Electronic Journal, 0, , .	0.4	0